

PAPER

## Mechanical behavior of HSLA350/440 and DP350/600 steels at different temperatures and strain rates

To cite this article: Claudimir J Rebeyka *et al* 2018 *Mater. Res. Express* **5** 066515

View the [article online](#) for updates and enhancements.

### Related content

- [A multiscale approach to modeling formability of dual-phase steels](#)  
A Srivastava, A F Bower, L G Hector Jr et al.
- [Effect of martensitic transformation on springback behavior of 304L austenitic stainless steel](#)  
H Fathi, H R Mohammadian Semnani, E Emadoddin et al.
- [Mechanical behavior of DP780 dual phase steel at a wide range of strain rates](#)  
Shengci Li, Lan Zhang, Hongjin Zhao et al.



**IOP | ebooks™**

Bringing you innovative digital publishing with leading voices to create your essential collection of books in STEM research.

Start exploring the collection - download the first chapter of every title for free.

# Materials Research Express



## PAPER

# Mechanical behavior of HSLA350/440 and DP350/600 steels at different temperatures and strain rates

RECEIVED  
5 April 2018

REVISED  
15 May 2018

ACCEPTED FOR PUBLICATION  
29 May 2018

PUBLISHED  
13 June 2018

Claudimir J Rebeyka<sup>1</sup> , Sergio T Button<sup>2</sup>, Sergio F Lajarin<sup>1</sup> and Paulo V P Marcondes<sup>1</sup>

<sup>1</sup> Universidade Federal do Parana–UFPR–Curitiba–Brazil

<sup>2</sup> Universidade Estadual de Campinas–UNICAMP, Campinas, Brazil

E-mail: [rebeyka@ufpr.br](mailto:rebeyka@ufpr.br)

**Keywords:** mechanical behavior, Hensel-Spittel, temperature, strain rate

## Abstract

The present paper presents an experimental investigation of the mechanical behavior of HSLA350/440 and DP350/600 through uniaxial tensile tests, covering temperatures from 30 °C to 800 °C, and strain rates from 0.035 s<sup>-1</sup> to 1.35 s<sup>-1</sup> encompassing several conditions for the motor vehicle parts manufacturing process. Experimental data were analyzed and tensile flow curves were plotted. Yield strength (YS), ultimate tensile strength (UTS), and total elongation (EL) were determined. A severe reduction of formability was found at 600 °C for both materials. At 800 °C, the UTS was dramatically reduced to around 100 MPa for both materials. No benefit was detected for HSLA350/440 in hot working. On the other hand, the EL of DP350/600 had a straight increase at 800 °C according to the strain rate. The Hensel-Spittel coefficients were calibrated for experimental data to represent the materials in a finite element (FE) code in order to predict the springback. Experimental deep drawing operations were performed, and the results showed good agreement with the simulations. As a result, the calibrated Hensel-Spittel constitutive equation can predict the mechanical behavior of HSLA350/440 and DP350/600 through simulations in a wide range of temperatures and strain rates.

## 1. Introduction

Nowadays, in order to reduce fuel consumption and vehicle emissions and improve lightness, the application of high strength steels (HSS) and advanced high strength steels (AHSS) became a commitment among vehicle manufacturers. Vehicle weight reduction is a key strategy used to decrease fuel consumption and reduce CO<sub>2</sub> emissions [1]. High strength steels such as high strength low alloy (HSLA) and dual-phase (DP) steels are alternatives to decrease the body weight of vehicles and, therefore, to reduce fuel consumption and emissions [2, 3].

Basically, HSLA steels consist of a ferrite matrix with fine carbides and nitrides, whereas DP steels consist of a ferrite matrix and martensite islands usually distributed along grain boundaries [4]. Generally, DP steels contain volume fractions from 20% to 30% of martensite and have a better formability than other HSLA steels with similar strength [5].

One of the major issues of high strength steels can be related to the springback effect on the dimensional accuracy of forming parts, as shown in figure 1. Thus, the correct prediction and control of springback effects are essential for the design of forming tools and processes, with no extra costs due to tool reworking [6].

On the other hand, the mechanical behavior of high strength steels can be directly related to the process temperatures and strain rates. Warm and hot stamping can result in parts with special features when compared to room temperature formed parts. The production of high strength steel components by warm and hot stamping requires a deep knowledge and control of the forming procedures [7].

Additionally, the proper design for warm and hot stamping process requires a deep knowledge both of the interface phenomena and the material behavior at different temperatures. However, the lack of knowledge on

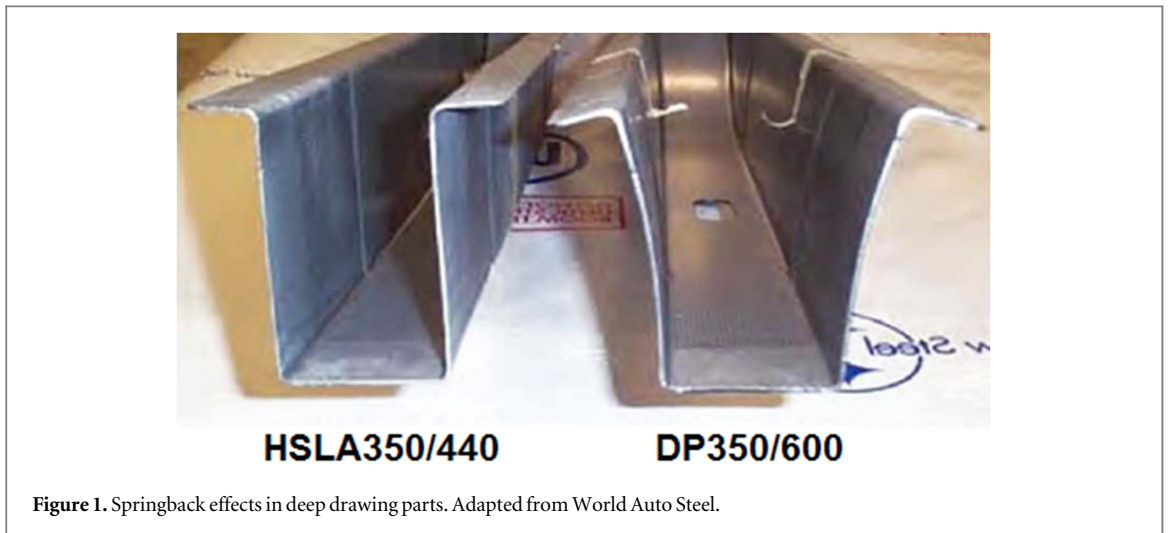


Figure 1. Springback effects in deep drawing parts. Adapted from World Auto Steel.

the mechanical behavior of materials in different temperatures is regarded as the main reason for the restricted application of warm and hot stamping in the industry [8].

In order to overcome springback problems, one must understand the material properties of the forming parts and their mechanical behavior under several process conditions. However, sheet manufacturers usually consider the mechanical properties of the material only under quasi-static loading at room temperature [4].

Recent research has aimed at understanding important aspects of formability in cold and hot forming, focusing on the material behavior and on the quality of the product. There are many constitutive equations for plastic flow stress related to strain, temperature, and strain rate [9]. The accurate modeling of the material rheological behavior is mandatory for an accurate FE model calibration [10, 11].

The model proposed by Hensel-Spittel can be used to represent the flow stress dependency on temperature and strain rate. It has one of the most complete constitutive equations for flow stress curves representation [10, 12]. This model can be used for a finite element (FE) code to predict the flow stress depending on different temperatures and strain rates [11, 13]. The Hensel-Spittel equation uses nine coefficients to describe the flow stress dependency on temperature and strain rate, equation (1).

$$\sigma = A e^{m_1 T} \varepsilon^{m_2} \dot{\varepsilon}^{m_3} e^{\frac{m_4}{\varepsilon}} (1 + \varepsilon)^{m_5} T e^{m_7 \varepsilon} \dot{\varepsilon}^{m_8} T^{m_9} \quad (1)$$

where  $\sigma$  is the scalar value of flow stress,  $\varepsilon$  is the equivalent true strain,  $\dot{\varepsilon}$  is the equivalent deformation rate, and  $T$  is the temperature. The coefficients are:  $A$ , Hensel-Spittel consistency coefficient;  $m_1$ , exponential temperature;  $m_2$ , strain hardening;  $m_3$ , strain rate hardening;  $m_4$ , strain softening;  $m_5$ , temperature strain;  $m_7$ , exponential strain hardening;  $m_8$ , exponential temperature-strain; and  $m_9$ , temperature coefficient [13].

In the present work, the constitutive flow stress curve relations for cold and hot forming were mathematically formulated using the Hensel-Spittel model. Although HSLA350/440 and DP350/600 steels have been designed for cold forming, the study of mechanical behavior under different temperatures and strain rates is very important. This may enhance the metal forming simulations in order to predict the springback effects of high strength steels at different process conditions.

In addition, there is a lack of information about the mechanical behavior of HSLA and DP steels at warm and hot temperatures, and different strain rates. Therefore, the aim of the present work was to study the mechanical behavior of HSLA350/440 and DP350/600 by uniaxial tensile tests covering different temperatures and strain rates. Experimental data from tensile flow curves have been used to calibrate the Hensel-Spittel constitutive equation for the FE code simulation. This code can predict the mechanical behavior of HSLA350/440 and DP350/600 for a wide range of strain rates and temperatures.

## 2. Materials

Two different steels were considered in the present study: HSLA350/440 and DP350/600. They were chosen because of their different springback effects in deep drawing parts, as shown in figure 1. Both materials were subjected to the same experimental conditions in order to evaluate the response of the Hensel-Spittel model to the springback prediction.

The mechanical behavior of these materials was investigated during the isothermal uniaxial tensile tests. Table 1 shows the chemical composition of the materials considered in the present study.

**Table 1.** Chemical composition (weight %).

Material	C	Mn	P	S	Si	Al	Ti	B
HSLA350/440	0.08	0.75	0.02	0.015	0.03	0.02	0.01	0.001
DP350/600	0.10	1.75	0.02	0.005	0.25	0.02	0.003	0.0005

**Table 2.** Mechanical properties on rolling direction under quasi-static loading at room temperature.

	t (mm)	YS (MPa)	UTS (MPa)	UE (%)	EL (%)
HSLA350/440	1.50	356	449	15	21
DP350/600	1.57	395	620	15	20

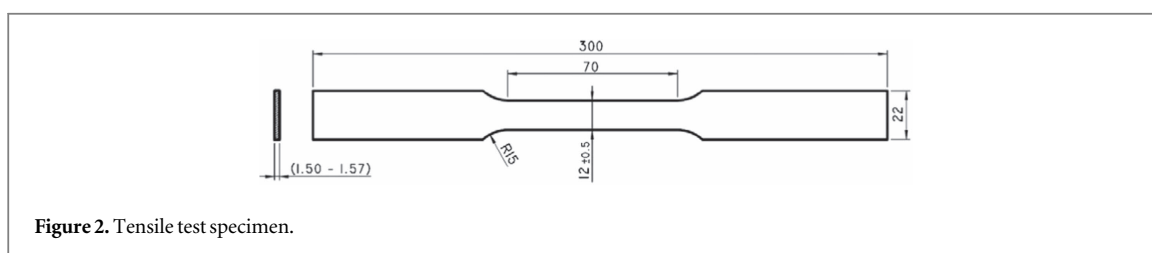
**Figure 2.** Tensile test specimen.

Table 2 shows the mechanical properties at room temperatures under quasi-static loading tests: thickness ( $t$ ), yield strength (YS), ultimate tensile strength (UTS), uniform elongation (UE), and total elongation (EL) were analyzed.

### 3. Experimental procedure

In order to investigate the mechanical behavior of the materials, isothermal uniaxial tensile tests of controlled temperatures and strain rates were conducted on 810-Flex Test 40 machine at the Laboratory of Mechanical Testing, University of Campinas, UNICAMP. Uniaxial tensile tests with controlled temperatures (heating, holding, test temperature, and cooling) and controlled crosshead speed were performed.

Thirty-six specimens in conformity with ASTM E8M-03 and ASTM E21-05 with average roughness  $R_a$  3.2  $\mu\text{m}$  and  $\pm 0 + .1$  mm linear tolerance were prepared, as shown in figure 2. Specimens were cut from the rolling direction (RD), diagonal direction (DD), and transverse direction (TD).

Specimens were heated one at a time, from room temperature to test temperatures of 30, 400, 600, and 800  $^{\circ}\text{C}$ , and held in the machine furnace for 10 min before the test. The tensile tests were performed at 2.5  $\text{mm s}^{-1}$  crosshead speed. For 800  $^{\circ}\text{C}$ , in order to evaluate the strain rate effects, there were different crosshead speeds (2.5  $\text{mm s}^{-1}$ , 25  $\text{mm s}^{-1}$ , and 100  $\text{mm s}^{-1}$ ), according to parameters shown in figure 3.

Each specimen was individually heated, held at the temperature inside the machine furnace and then submitted to uniaxial tensile in order to test rupture. At least one repetition of each test was performed to confirm the results.

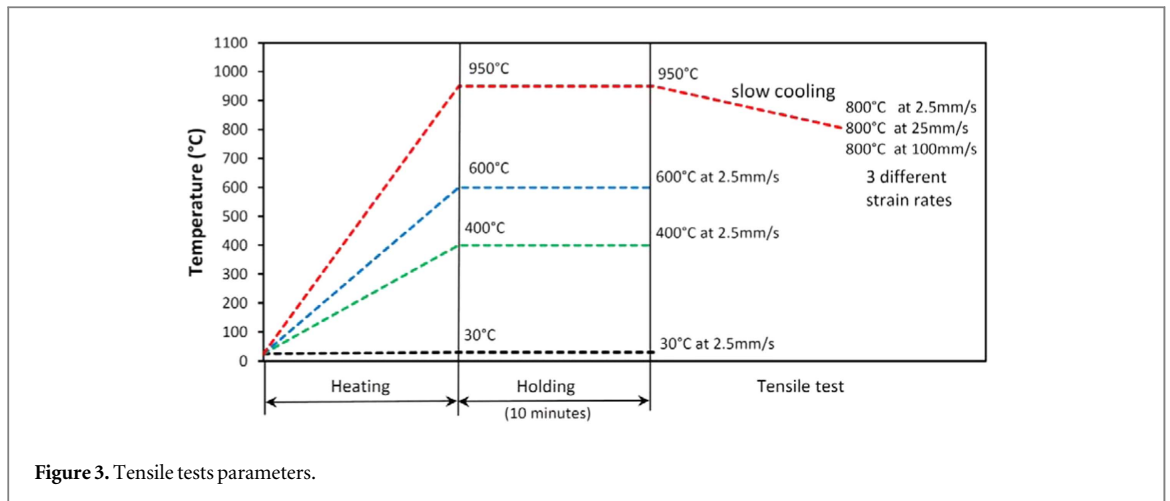
For 30, 400, and 600  $^{\circ}\text{C}$ , the specimens were heated straight to the test temperature and held at that temperature for 10 min. After this, they were tested to rupture at 2.5  $\text{mm s}^{-1}$  crosshead speed. For 800  $^{\circ}\text{C}$ , the specimens were first heated and held at 950  $^{\circ}\text{C}$  for 10 min for austenitization. After this, they were slowly cooled down to 800  $^{\circ}\text{C}$  before tensile tests at three different crosshead speeds.

### 4. Experimental results and discussions

Each tensile test condition leads to a specific strain rate obtained from the ratio between the final and the initial length of the specimen. The results are shown in table 3.

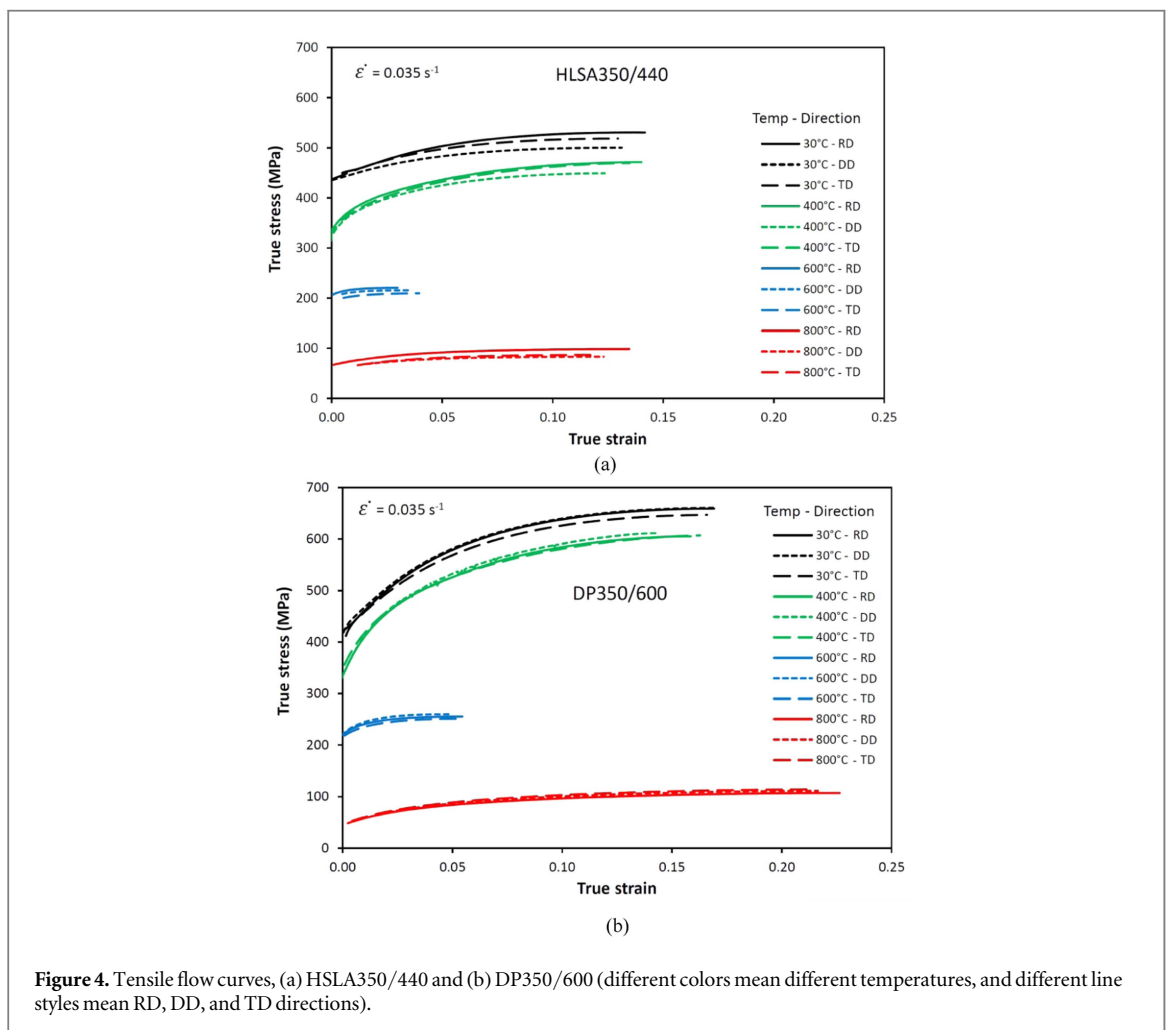
Considering the 2.5  $\text{mm s}^{-1}$  crosshead speed, all strain rates can be rounded to the same double-digit value for all temperatures. In this case, experimental data from tensile flow curves at the strain rate of 0.035  $\text{s}^{-1}$  were plotted in figure 4.

At 30  $^{\circ}\text{C}$ , the following results were found: HSLA350/440 with UTS of 500 MPa and EL between 0.13 and 0.15, and DP350/600 with UTS of 650 MPa and EL between 0.15 and 0.20. These amounts are a little higher than the information provided by the manufacturer, probably due to the crosshead speeds. In the present analysis, the



**Table 3.** Strain rates dependency on temperature and crosshead speeds.

	30 °C 2.5 mm s <sup>-1</sup>	400 °C 2.5 mm s <sup>-1</sup>	600 °C 2.5 mm s <sup>-1</sup>	800 °C 2.5 mm s <sup>-1</sup>	800 °C 25 mm s <sup>-1</sup>	800 °C 100 mm s <sup>-1</sup>
HSLA350/440	0.0347	0.0349	0.0346	0.0347	0.3154	1.2537
DP350/600	0.0346	0.0351	0.0346	0.0351	0.3147	1.2496



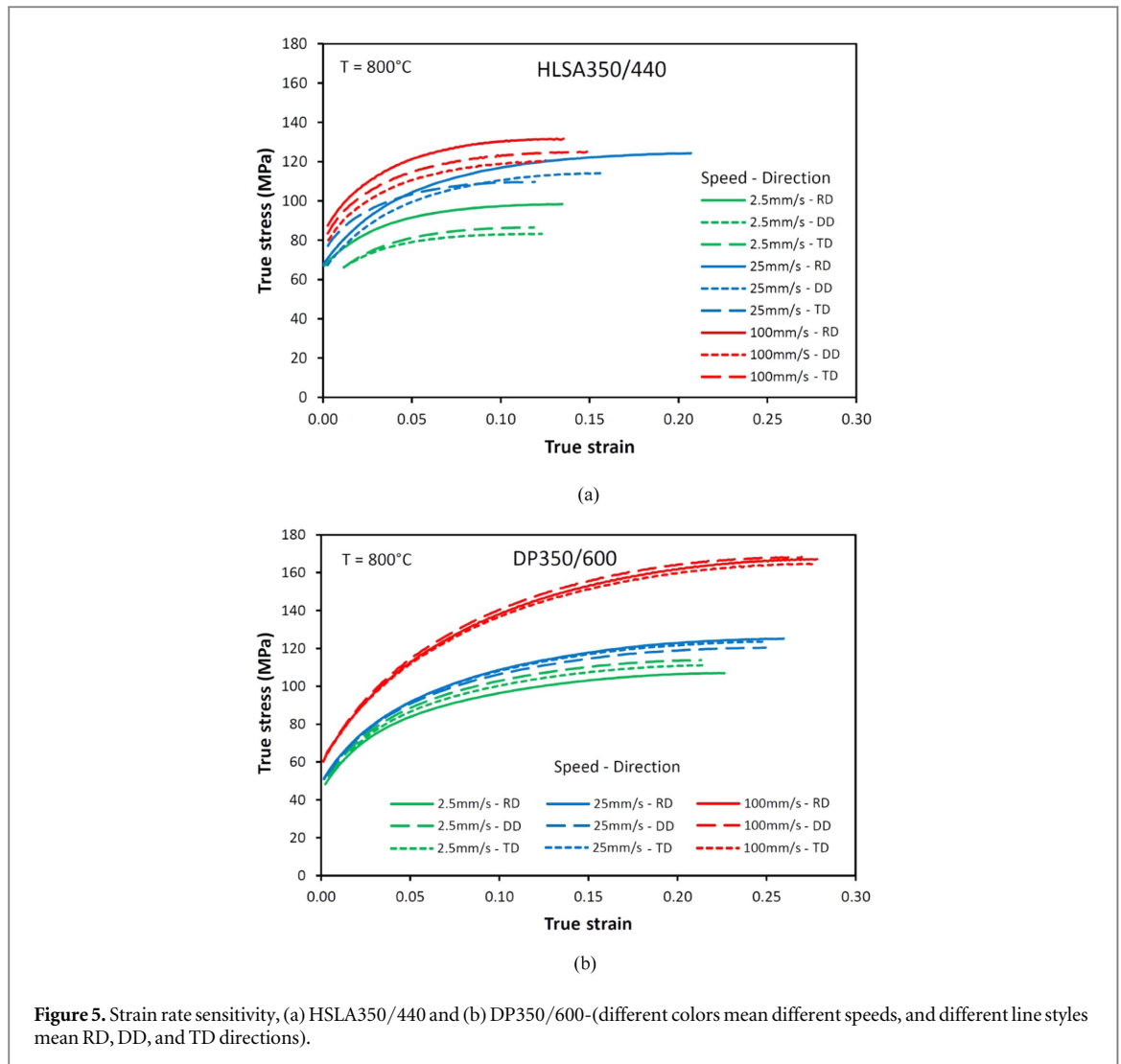


**Figure 5.** Strain rate sensitivity, (a) HSLA350/440 and (b) DP350/600-(different colors mean different speeds, and different line styles mean RD, DD, and TD directions).

machine crosshead speed was set to  $2.5 \text{ mm s}^{-1}$ , which leads to the strain rate of  $0.035 \text{ s}^{-1}$ . Both materials showed a little reduction of UTS at  $400 \text{ }^{\circ}\text{C}$ , but almost the same EL when compared to  $30 \text{ }^{\circ}\text{C}$ .

However, a noticeable reduction of UTS and EL properties was found at  $600 \text{ }^{\circ}\text{C}$  for both materials. All specimens tested at this temperature showed properties with UTS under 300 MPa, and EL under 0.05. This EL behavior leads to a severe reduction of formability, which was unexpected in the present study. As a result, further investigation will be required. Therefore, for similar cases, forming operations of HSLA350/440 and DP350/600 to  $600 \text{ }^{\circ}\text{C}$  processing temperature should be avoided.

At  $800 \text{ }^{\circ}\text{C}$ , the UTS was dramatically reduced to around 100 MPa for both materials. Specifically, HSLA350/440 at  $800 \text{ }^{\circ}\text{C}$  showed almost the same EL when compared to  $30 \text{ }^{\circ}\text{C}$ , reinforcing that it presents no benefit in hot working. In contrast, DP350/600 at  $800 \text{ }^{\circ}\text{C}$  showed higher EL when compared to  $30 \text{ }^{\circ}\text{C}$ , increasing formability.

The matching the flow curves for different cutting directions (RD, DD, and TD) suggests that both materials are virtually isotropic for any specific temperature. The isotropic behavior is enhanced to higher temperatures for the flow curves almost fit one another. The results of DP350/600 at  $800 \text{ }^{\circ}\text{C}$  show very close flow curves for RD, DD, and TD.

For strain rate sensitivity (m) analysis, each specimen was heated to  $950 \text{ }^{\circ}\text{C}$  and held at that temperature for 10 min for austenitization. The specimen was slowly cooled down to  $800 \text{ }^{\circ}\text{C}$  inside the machine furnace, and tensile tests were performed at  $2.5 \text{ mm s}^{-1}$ ,  $25 \text{ mm s}^{-1}$ , and  $100 \text{ mm s}^{-1}$ . Figure 5 shows the flow curves at  $800 \text{ }^{\circ}\text{C}$  for different crosshead speeds, according to the cutting direction of the specimens.

Both materials showed UTS increase as the strain rate went up. No substantial effects on EL of HSLA350/440 were found for different strain rates. On the other hand, the EL of DP350/600 underwent a direct increase according to the strain rate. The flow curves for different cutting directions (RD, DD, and TD) suggest that both materials had virtually an isotropic behavior for any specific strain rate.

At  $800 \text{ }^{\circ}\text{C}$ , both HSLA350/440 and DP350/600 present an increase in the yield strength due to the increase in the strain rates from  $0.035 \text{ s}^{-1}$  to  $1.25 \text{ s}^{-1}$  (figure 6).

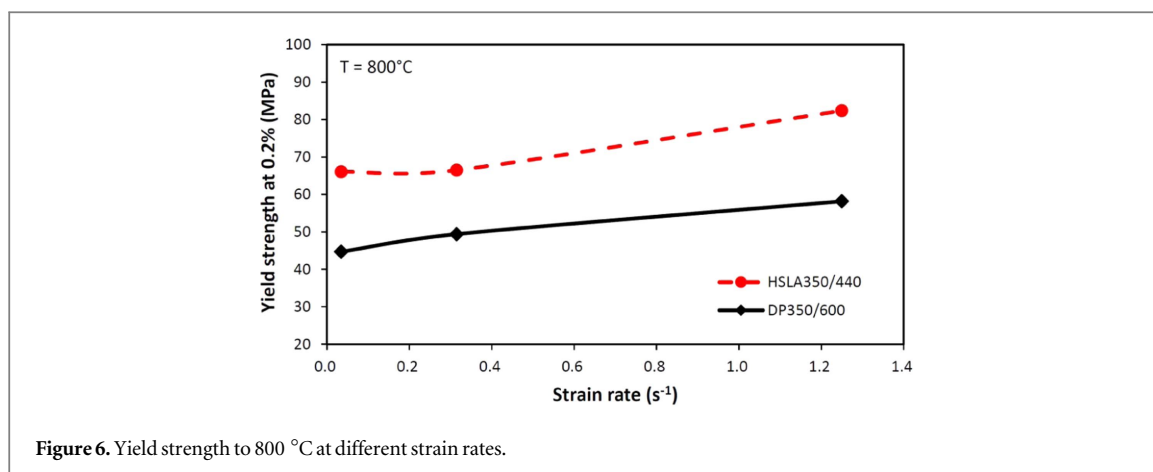


Figure 6. Yield strength to 800 °C at different strain rates.

Table 4. Hensel-Spittel adjusted coefficients.

Coefficient	HSLA350/440	DP350/600
A	0.005 44	0.005 32
$m_1$	0.007 06	0.006 38
$m_2$	0.049 44	0.139 96
$m_3$	-2.822 39	-2.819 79
$m_4$	2.955E-6	1.018E-4
$m_5$	8.170E-4	8.358E-5
$m_7$	0.147 62	-0.171 28
$m_8$	0.003 60	0.003 60
$m_9$	0.659 44	0.795 06

The Hensel-Spittel coefficients were calibrated to the experimental data via non-linear regression in the OriginPro® V2016–b9.3.2.303 software, at a 95% confidence level. Table 4 shows these adjusted coefficients.

Figure 7 shows the experimental data and the calibrated Hensel-Spittel equation. Experimental data are presented in solid lines, the calibrated Hensel-Spittel's are presented in dots.

The Hensel-Spittel equation was adequate to HSLA350/440 and DP350/600 experimental data with the adjusted coefficients. For different temperatures and strain rates, the Hensel-Spittel model is in good agreement with the experimental data.

A deep drawing numerical simulation on the FE code ABAQUS 6.14 was built to validate the present study. The flow stress data were generated through the calibrated Hensel-Spittel equation. The springback prediction was compared to experimental deep drawing springback effects.

Simulations covering different temperatures (30, 400, and 600 °C) and different stroke speeds (2.5 mm s<sup>-1</sup> and 15 mm s<sup>-1</sup>) were performed - within the experimental possibilities provided by the laboratory. Figure 8 shows the results of simulation and experimental procedures.

The springback effects decrease as temperature rises. There was no substantial reduction for different stroke speeds. Simulations are in good agreement with the experimental data. The comparison of simulation and experimental results show that the Hensel-Spittel calibrated equation can satisfactorily predict the mechanical behavior of HSLA350/440 and DP350/600 for simulations on several forming conditions.

## 5. Conclusions

The experimental results can describe the HSLA350/440 and DP350/600 mechanical behavior for temperatures from 30 °C to 800 °C, and strain rates from 0.035 s<sup>-1</sup> to 1.35 s<sup>-1</sup>. A severe reduction of formability was found at 600 °C, deserving further investigation. At 800 °C, the UTS was dramatically reduced to around 100 MPa for both materials. There is no benefit in using HSLA350/440 in hot working. On the other hand, the EL of DP350/600 increases at 800 °C according to strain rate. The Hensel-Spittel constitutive equation was adequate for experimental data. The calibrated Hensel-Spittel constitutive equation can predict the mechanical behavior of HSLA350/440 and DP350/600 in a wide range of working temperatures and strain rates. Although HSLA350/440 and DP350/600 steels have been designed for cold forming, the study of mechanical behavior at different

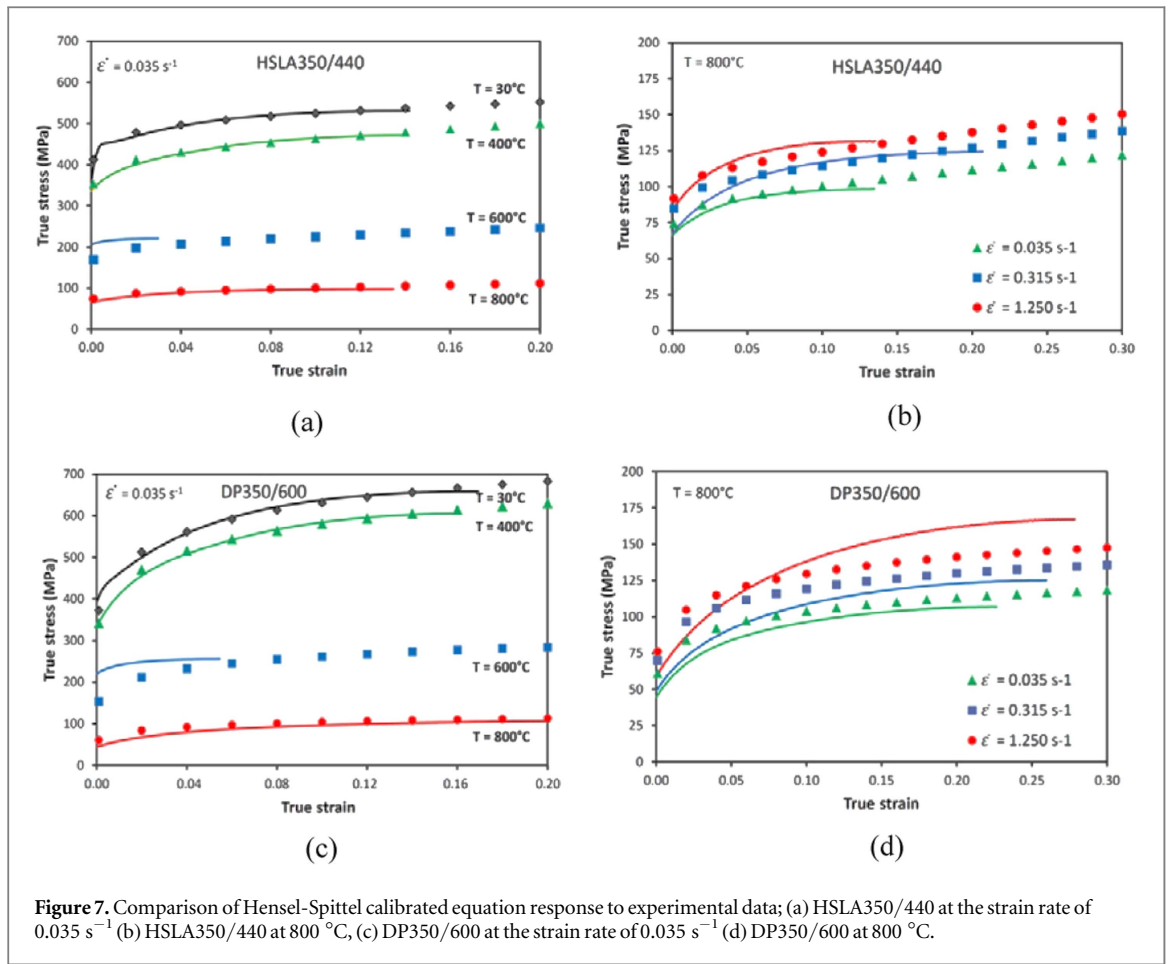


Figure 7. Comparison of Hensel-Spittel calibrated equation response to experimental data; (a) HSLA350/440 at the strain rate of  $0.035 \text{ s}^{-1}$  (b) HSLA350/440 at  $800^\circ\text{C}$ , (c) DP350/600 at the strain rate of  $0.035 \text{ s}^{-1}$  (d) DP350/600 at  $800^\circ\text{C}$ .

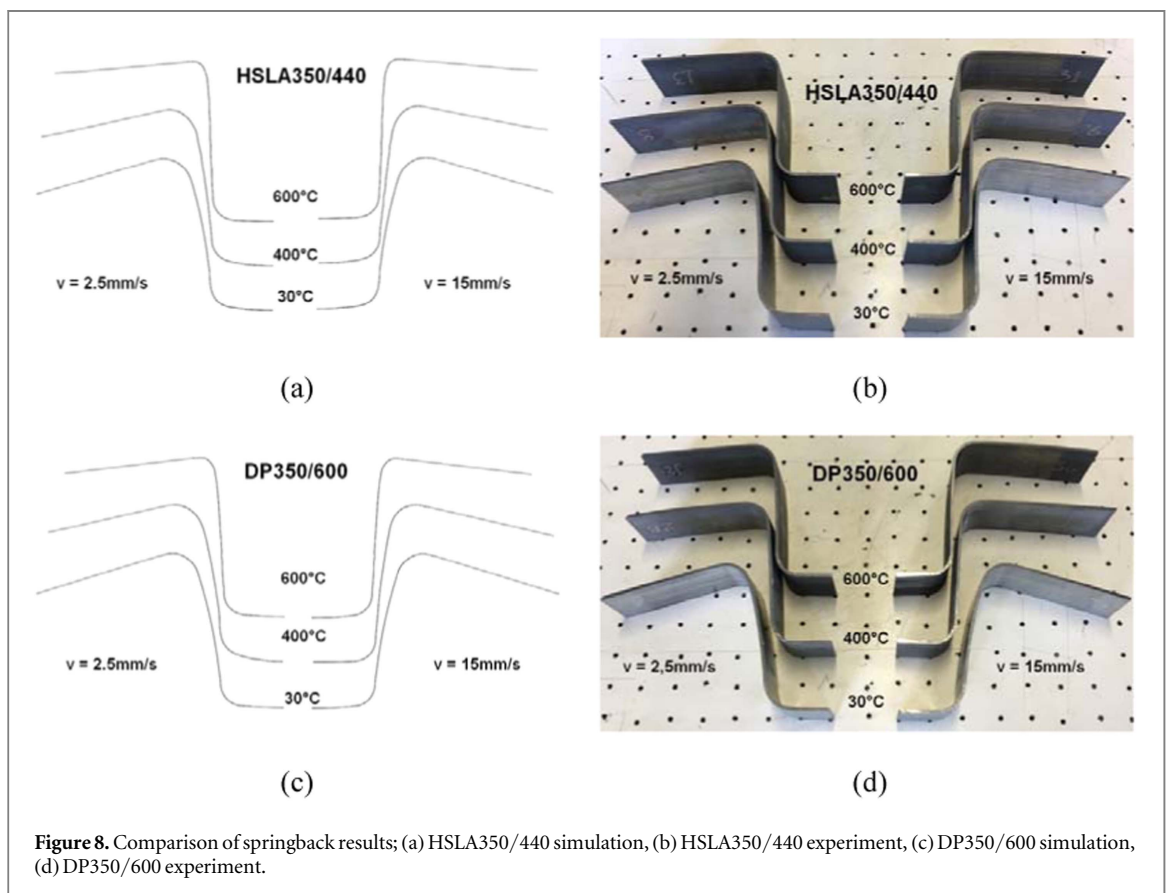


Figure 8. Comparison of springback results; (a) HSLA350/440 simulation, (b) HSLA350/440 experiment, (c) DP350/600 simulation, (d) DP350/600 experiment.



temperatures and strain rates may enhance the metal forming simulations in order to predict the springback effects to high strength steels in different conditions of vehicle parts production.

## Acknowledgments

The authors thank the FAPESP (Proc. 09/54138-8) for the support for the tensile tests, the ArcelorMittal for supplying the HSLA350/440 and DP350/600 samples for the present work. We also thank the CNPQ Agency (Brazil) for a grant.

## ORCID iDs

Claudimir J Rebeyka  <https://orcid.org/0000-0002-9935-0136>

## References

- [1] Jia Q, Guo W, Li W, Zhu Y, Peng P and Zou G 2016 *J. Mater. Process. Technol.* **236** 73
- [2] Chen X, Huang Y and Lei Y 2015 *J. Alloys Compd.* **631** 225
- [3] Cao Y, Karlsson B and Ahlström J 2015 *Materials Science and Engineering* **A636** 124
- [4] Ozturk F, Polat A, Toros S and Picu R C 2013 *Journal of Iron and Steel Research, International* **20** 68
- [5] Oliver S, Jones T B and Fournalaris G 2007 *Mater. Sci. Technol.* **A507** 423
- [6] Keeler S, Kimchi M and Mooney P J 2017 *Advanced High Strength Steels Application Guidelines* Version 6.0 WorldAutoSteel <https://www.worldautosteel.org/projects/advanced-high-strength-steel-application-guidelines/>
- [7] Karbasian H and Tekkaya A E 2010 *J. Mater. Process. Technol.* **210** 2103
- [8] Turreta A, Bruschi S and Ghiotti A 2006 *J. Mater. Process. Technol.* **177** 396
- [9] Kim J H, Kim D, Han H N, Barlat F and Lee M G 2013 *Materials Science and Engineering* **23** 222
- [10] Meyer L, Weise A and Hahn F 1997 *Journal de Physique IV Colloque* **07** 13
- [11] Tang B T, Bruschi S, Ghiotti A B and Bariani P F 2016 *J. Mater. Process. Technol.* **228** 76
- [12] Hensel A and Spittel T 1978 Kraft- und arbeitsbedarf. Bildsomer formgebungs verfahren VEB Deutscher Verlag fur Grundstoffindustrie. Lipsk 528
- [13] Novella M F, Ghiotti A, Bruschi S and Bariani P F 2015 *J. Mater. Process. Technol.* **222** 259